Biomaterials 33 (2012) 7489–7496

Contents lists available at SciVerse ScienceDirect

Biomaterials

journal homepage: www.elsevier.com/locate/biomaterials

The role of nacreous factors in preventing osteoporotic bone loss through both osteoblast activation and osteoclast inactivation

Hyunsoo Kim [a,1,2], Kyunghee Lee [a,1], Chang-Yong Ko [b], Han-Sung Kim [c], Hong-In Shin [d], Taesoo Kim [e], Seoung Hoon Lee [f], Daewon Jeong [a,*]

[a] Department of Microbiology, Aging-Associated Vascular Disease Research Center, Yeungnam University College of Medicine, 317-1 Daemyung-Dong, Nam-Gu, Daegu 705-717, Republic of Korea
[b] Inspection and Diagnosis Methods, Fraunhofer Institute for Nondestructive Testing, Dresden 01109, Germany
[c] Department of Biomedical Engineering, Institute of Medical Engineering and Yonsei-Fraunhofer Medical Device Laboratory, Yonsei University, Wonju 220-710, Republic of Korea
[d] IHBR, Department of Oral Pathology, School of Dentistry, Kyungpook National University, Daegu 700-412, Republic of Korea
[e] Center for Herbal Medicine Improvement Research, Korea Institute of Oriental Medicine, Daejeon 305-811, Republic of Korea
[f] Department of Oral Microbiology and Immunology, Wonkwang University School of Dentistry, Iksan 570-749, Republic of Korea

ARTICLE INFO

Article history:
Received 1 May 2012
Accepted 30 June 2012
Available online 16 July 2012

Keywords:
Nacre
Bone remodeling
Osteoporosis
Biocompatibility

ABSTRACT

Excessive bone resorption by osteoclasts relative to bone formation by osteoblasts results in the development of osteoporosis. Anti-osteoporotic agents that are able both to inhibit bone resorption and to stimulate bone formation are not available. We now show that water-soluble nacreous factors prepared from the pearl oyster *Pteria martensii* prevent osteoporotic bone loss associated with estrogen deficiency in mice mainly through osteoclast inactivation. Nacreous factors stimulated osteoblast biomineralization *in vitro* in association with activation of signaling by c-Jun NH_2-terminal kinase (JNK) and Fos-related antigen-1 (Fra-1). They also suppressed both osteoclast formation by blocking up-regulation of nuclear factor of activated T cells cytoplasmic 1 (NFATc1) as well as bone pit formation mediated by mature osteoclasts, likely by disrupting the actin ring of these cells. Our findings thus show that the components of a natural material have beneficial effects on bone remodeling that are mediated through regulation of both osteoblast and osteoclast function. They may thus provide a basis for the development of biomimetic bone material as well as anti-osteoporotic agents.

1. Introduction

Bone is a dynamic tissue that provides mechanical support and physical protection of soft tissues in the vertebrate body as well as serves as a mineral reservoir to supply the needs of other tissues [1]. Bone consists of an organic protein matrix as well as inorganic hydroxyapatite formed by the crystallization of calcium and phosphate, and it undergoes continuous remodeling, in which old bone is replaced with new, throughout life [2]. Such remodeling depends on precise coupling between the actions of bone-resorbing osteoclasts and bone-forming osteoblasts and requires multicellular communication in the bone marrow microenvironment. The receptor activator of the NF-κB ligand (RANKL), expressed by osteoblasts, immune T cells and endothelial cells, activates osteoclast formation by binding to its cognate receptor RANK which is present on the cytoplasmic membrane of osteoclast precursors [3,4]. Otherwise, osteoprotegerin produced from osteoblasts blocks osteoclast formation by inhibiting the interaction between RANKL and RANK [3,5]. Interferon gamma and interleukin 4 expressed and secreted from T cells also suppress osteoclast formation by blocking RANKL/RANK signaling [3]. Conversely, osteoclast-derived coupling factors, such as transforming growth factor beta, bone morphogenetic proteins, insulin-like growth factors, vacular H^+-ATPase V0 domain subunit d2 and Ephrin B2, stimulate osteoblastic bone formation [5]. Moreover, there exists an inverse relationship between osteoblast and adipocyte differentiation in bone regeneration by platelet-rich plasma [6].

Osteoclastic bone resorption involves mineral dissolution and matrix protein degradation [2,7]. This is followed by osteoblastic bone formation, which involves the newly formed matrix and mineral deposition, leading to bone homeostasis. An uncoupled balance between bone resorption and bone formation causes bone diseases, particularly in osteoporosis. Estrogen deficiency caused by

* Corresponding author. Tel.: +82 53 620 4365; fax: +82 53 653 6628.
E-mail address: dwjeong@ynu.ac.kr (D. Jeong).
[1] Both authors contributed equally to this study.
[2] Present address: Department of Pathology and Laboratory Medicine, University of Pennsylvania, School of Medicine, Philadelphia, PA 19104, USA.

0142-9612/$ – see front matter © 2012 Elsevier Ltd. All rights reserved.
http://dx.doi.org/10.1016/j.biomaterials.2012.06.098

menopause results in a 'high turnover' bone loss due to both excessive osteoclastic bone resorption and reduced or insufficient osteoblastic bone formation [7–9]. In contrast, the senescence-accelerated mouse (SAMP6) and Klotho (aging suppressor gene)-deficient mouse exhibit low bone formation due to reduced osteoblastogenesis and bone resorption, respectively, leading to 'low turnover' bone loss [10,11]. Anti-resorptive agents, such as bisphosphonates and the anti-RANK-ligand monoclonal antibody AMG162, and anabolic agents, such as parathyroid hormone and the anti-sclerostin monoclonal antibody, have emerged as potential therapeutic drugs for the treatment of osteoporotic bone loss [7]. Furthermore, the development of formulations for the treatment or prevention of osteoporotic disorders will likely require the combination of agents that inhibit bone resorption and induce bone formation.

Natural products analogous to bone might be expected to contain bioactive molecules able to promote biomineralization and to stimulate bone formation by osteoblasts. One such product, nacre (also known as mother of pearl), consists of 95–99% crystalline calcium carbonate (aragonite) and 1–5% organic matrix [12,13]. Although nacre and bone differ in mineral composition and the ratio of organic matrix to minerals [12–14], they are similar in that they both consist of a composite mineralized matrix with a well-organized microstructure and in that they both serve to protect soft tissues from external impact [1,15]. Studies have suggested that powdered nacre is biocompatible with bone tissue and stimulates osteoblasts when implanted in rats, sheep, or humans [16–18]. *In vitro* experiments have also shown that organic matrix fractionated from water-soluble nacre components by distinct approaches is capable of stimulating biomineralization by osteoblasts [19,20] as well as of inhibiting osteoclastic bone resorption through suppression of cathepsin K activity [21].

Although several studies have independently reported a possible action of nacre in osteoblastic bone formation and osteoclastic bone resorption, no directly coordinated evidence between nacre and bone remodeling has been demonstrated. The aim of this study was to investigate the effects of water-soluble nacreous factors (WSNF) on bone remodeling both in an ovariectomized (OVX)-induced osteoporotic mouse model and in an osteoblast and osteoclast cell culture system.

2. Materials and methods

2.1. Reagents

α-Minimum essential medium (α-MEM), fetal bovine serum (FBS), antibiotics, and trypsin-EDTA were obtained from Hyclone (Logan, UT, USA). Macrophage colony-stimulating factor (M-CSF) and RANKL were kindly provided by Yongwon Choi (University of Pennsylvania). Ascorbic acid, β-glycerophosphate, hematoxylin, eosin, alizarin red S, cetylpyridinium chloride, and fluorescein isothiocyanate-conjugated phalloidin were obtained from Sigma–Aldrich (St. Louis, MO, USA). Antibodies to phosphorylated ERK (Thr^{202}/Tyr^{204}), to phosphorylated p38 (Thr^{180}/Tyr^{182}), to phosphorylated JNK (Thr^{183}/Tyr^{185}), to phosphorylated IκBα (Ser^{32}), to ERK, to p38, and to JNK were from Cell Signaling Technology (Frankfurt, Germany), and those to NFATc1, to c-Src, to c-Fos, to ALP, to Fra-1, to HA, and to β-actin were from Santa Cruz Biotechnology (Santa Cruz, CA, USA). Unless indicated otherwise, all other reagents were from Sigma–Aldrich.

2.2. Preparation of WSNF

WSNF were prepared as described previously [22]. In brief, the powdered nacre from the inner part of the shell of *Pteria martensii* was suspended in distilled water in a final concentration of 4 and 500 mg/ml, and subjected to extraction by incubation for 12 h at room temperature with rocking. The suspension was centrifuged at 3000 × *g* for 30 min at room temperature, and the resulting water-soluble fraction was sterilized by passage through a syringe filter with a pore size of 0.22 μm. Powdered nacre and WSNF were administrated orally to mice at a dose of 25 mg/kg per day and at the volume of two hundred microliters of stock solution extracted from 4 mg/ml powdered nacre per day, respectively. Cells in culture were treated with a twentieth part of WSNF extracted from 500 mg/ml powdered nacre. The calcium concentration of WSNF prepared from 4 mg/ml and 500 mg/ml as measured with the use of a QuantiChrome Calcium Assay Kit (BioAssay Systems, Hayward, CA, USA) was 2.24 μM and 280 μM, respectively. Calcium at these concentrations dissolved from $CaCO_3$, the major component of nacre, was used as a control.

2.3. Ovariectomy and histomorphometric analyses

Eight-week-old female ddY mice (Central Lab Animals, Seoul, Korea) were anesthetized by intraperitoneal injection of Avertin and subjected to bilateral ovariectomy or sham surgery, as described previously [23]. Powdered nacre or WSNF were administered orally and daily to the mice for 30 days beginning 3 days after surgery, and the animals were then sacrificed for analysis. For trabecular morphometry, the proximal tibia was scanned in three dimensions by high-resolution micro-computed tomography (1076 μCT System; Skyscan, Aartselaar, Belgium). Bone indices including bone mineral density (BMD), bone volume as a percentage of total bone volume (BV/TV), and trabecular number (Tb.N) were determined from the micro-computed tomography (μCT) data. For analysis of bone histology, 5-μm-thick sagittal sections were stained with hematoxylin-eosin to detect osteoblasts and for tartrate-resistant acid phosphatase (TRAP) to visualize osteoclasts. Sections were counterstained with methylene blue. For analysis of mineral apposition rate (MAR) and bone formation rate (BFR), mice were injected intraperitoneally with calcein (15 mg/kg) both 10 and 3 days before they were killed at 30 days after the initial administration of WSNF. After the end of the tibia was cut into section ~20 μm thick using a grinding, the calcein double-labeled bone surface was photographed to measure MAR and BFR. All animal experiments were approved by the Institutional Animal Care and Use Committee of Yeungnam University College of Medicine.

2.4. Osteoblast biomineralization

Primary osteoblast precursors were prepared from the calvaria of newborn C57BL/6J mice (Central Lab Animals) by five sequential digestions with 0.2% dispase II and 0.1% collagenase type IA. Cells isolated in fractions 2–5 were pooled and cultured until they achieved 90% confluence in α-MEM supplemented with 10% FBS. For examination of mineralized nodule formation, osteoblast precursors (1×10^4 cells per well in 48-well plates) were cultured in osteogenic medium [α-MEM supplemented with 10% FBS, 10 mM β-glycerophosphate, and ascorbic acid (100 μg/ml)] for 6 days with a change of medium after 3 days and were then stained with 2% alizarin red S (pH 4.2) to visualize the nodules. The stained cells were then washed with distilled water before elution of the dye with 10% cetylpyridinium chloride and measurement of its absorbance at 595 nm with a microplate reader (Bio-Rad, Hercules, CA, USA). For measurement of ALP activity, osteoblast precursors (5×10^6 cells per well in six-well plates) were cultured in osteogenic medium for 6 days, washed with ice-cold phosphate-buffered saline, suspended in a lysis buffer [10 mM Tris–HCl (pH 8.2), 2 mM $MgCl_2$, 0.05% Triton X-100], frozen and thawed twice, and subjected to several rounds of ultrasonic treatment. The cell lysates were centrifuged to remove debris, and the resulting supernatants (200 μg of protein) were incubated for 30 min at 37 °C in an assay mixture containing 0.1 M sodium carbonate buffer (pH 10), 10 mM *p*-nitrophenyl phosphate, and 1 mM $MgCl_2$. The reaction was terminated by the addition of NaOH to a final concentration of 0.1 M. The amount of *p*-nitrophenol generated in the assay mixture was determined by measurement of absorbance at 405 nm with a microplate reader.

2.5. Osteoclast differentiation, bone pit formation, and F-actin staining

Bone marrow–derived mononuclear osteoclast precursors were prepared from the tibia and femur of 6-week-old male C57BL/6J mice as described [24]. Cells (1×10^4 cells per well in 48-well plates) were induced to differentiate into osteoclasts in α-MEM supplemented with M-CSF (30 ng/ml) and RANKL (25 ng/ml) for 5 days, fixed, and stained for TRAP with the use of a leukocyte acid phosphatase staining kit (Sigma–Aldrich). TRAP-positive cells with 10 or more nuclei were counted with the use of a light microscope. A TRAP solution assay was examined by addition of 5.5 mM *p*-nitrophenyl phosphate, a colorimetric substrate, in the presence of 10 mM sodium tartrate (pH 5.2). Absorbance was measured at 405 nm using a microplate reader. For assay of osteoclast function, osteoclast precursors (5×10^3 cells per well in 96-well plates) were seeded on dentine slices (IDS Ltd., Boldon, UK) and induced to differentiate into osteoclasts by culture with M-CSF and RANKL, after which they had achieved 70–80% confluence. The cells were then exposed to WSNF for 2 days before their removal from the dentine slices by ultrasonic treatment, and the slices were stained with hematoxylin for 1 min for measurement of the resorbed area of pits with the use of a light microscope and Image-Pro Plus version 6.0 software (MediaCybernetics). For detection of the actin ring, mature osteoclasts were exposed to WSNF for 2 days, fixed with 3.7% formalin, permeabilized with 0.1% Triton X-100 in phosphate-buffered saline, and stained with fluorescein isothiocyanate-conjugated phalloidin. Fluorescence images were captured with an Olympus BX51 fluorescence microscope.

2.6. Retrovirus preparation and infection

A retroviral vector for a hemagglutinin epitope (HA)-tagged constitutively active form of NFATc1 (pMX-Ca-NFATc1) as well as a control vector (pMX) were described

previously [25] and were introduced into PLAT-E packaging cells by transfection for 3 days with the use of polyethyleneimine (Polysciences, Warrington, PA, USA). The culture medium containing retroviruses was harvested and passed through a 0.22-μm syringe filter. Osteoclast precursors were infected with control or Ca-NFATc1 retroviruses for 6 h in the presence of M-CSF (120 ng/ml) and polybrene (5 μg/ml) and were then subjected to selection with puromycin (2 μg/ml) for 2 days in the presence of M-CSF (120 ng/ml). Puromycin-resistant cells were induced to undergo osteoclast differentiation.

2.7. Reverse transcription-polymerase chain reaction (RT-PCR) and immunoblot analyses

For RT-PCR analysis, total RNA was extracted from cells with the use of the Trizol reagent (Invitrogen, Carlsbad, CA), and 3 μg of the RNA were subjected to RT followed by PCR with the use of a Thermo Hybaid PCR Express system (Thermo Hybaid, Ulm, Germany). PCR primers were synthesized by Bionics (Seoul, Korea), and their sequences are listed in Supplementary Table S1. For immunoblot analysis, cells were washed three times with ice-cold phosphate-buffered saline, resuspended in a lysis buffer [20 mM Tris–HCl (pH 7.5), 150 mM NaCl, 1% Nonidet P-40, 0.5% sodium deoxycholate, 1 mM EDTA, 0.1% SDS, 1 mM NaF, 2 mM Na_3VO_4, 1 mM β-glycerophosphate, and protease inhibitor cocktail (Roche, Munich, Germany)]. Cell lysates were centrifuged to remove debris, and the resulting supernatants (10–30 μg of protein) were fractionated by SDS-polyacrylamide gel electrophoresis on a 10% gel. The separated proteins were transferred to a polyvinylidene difluoride membrane before exposure to primary antibodies. Immune complexes were detected with West SaveUp chemiluminescence substrate (Abfrontier, Seoul, Korea). Band intensity was determined by densitometric analysis software (Image-Pro Plus version 6.0).

2.8. Statistical analysis

For statistical analysis, all data were presented as means ± SD from at least three independent experiments. Data with more than three groups were assessed by analysis of variance (ANOVA) using the SPSS 18.0 software package. When significant differences were found, the two-tailed Student's *t* test was used to compare data between two groups. A *P* value of <0.05 was considered statistically significant.

3. Results

3.1. Administration of the powdered nacre and WSNF to osteoporotic mice

We prepared powdered nacre by grinding the inner layer of the shell of the pearl oyster *P. martensii* and then extracted WSNF from the powder. To examine the possible effects of the powdered nacre and WSNF on bone remodeling, we administered each material orally at a concentration which is estimated to be efficacious in the treatment of osteoporotic patients by experienced practitioners of oriental medicine for 30 days to OVX or sham-operated mice. High-resolution μCT revealed that both materials ameliorated the osteoporotic characteristics associated with estrogen deficiency, including the decreases in bone mineral density (BMD), in trabecular bone volume as a percentage of total bone volume (BV/TV), and in trabecular number (Tb.N) (Fig. 1). The effects of WSNF were slightly greater than those of powdered nacre, but the differences were not statistically significant.

3.2. Effects of WSNF on osteoblast and osteoclast formation in vivo

Analysis of the inorganic and organic components of WSNF revealed the presence of sodium, calcium, potassium, phosphorus, iron, and zinc as well as lipid and protein (Supplementary Table S2). To assess the possibility that calcium and other additive factors in WSNF are responsible for the observed effects on bone remodeling [26], we prepared a solution containing an identical concentration of calcium dissolved from $CaCO_3$, the major component of nacre, as a control for subsequent *in vivo* experiments. Whereas calcium slightly inhibited OVX-induced bone loss, which corresponded to a statistically significant difference, its effects were much less pronounced than were those of WSNF (Fig. 2A). We also found that MAR and BFR in OVX mice treated with WSNF were restored to the normal level of sham-operated animals, whereas calcium had a much smaller effect on this parameter (Fig. 2B). Thus, these results indicated that calcium alone cannot wholly account for the effects of WSNF on bone loss and WSNF must contain other factors in addition to calcium to regulate bone remodeling. We next examined osteoblast and osteoclast formation on the surface of trabecular bone. The bone recovery promoted by WSNF was associated with a decrease in the number of osteoclasts in OVX mice (Fig. 2C). Although the number of osteoblasts appeared to be slightly increased after treatment of WSNF, it was not significant statistically. Together, these findings suggested that prevention of

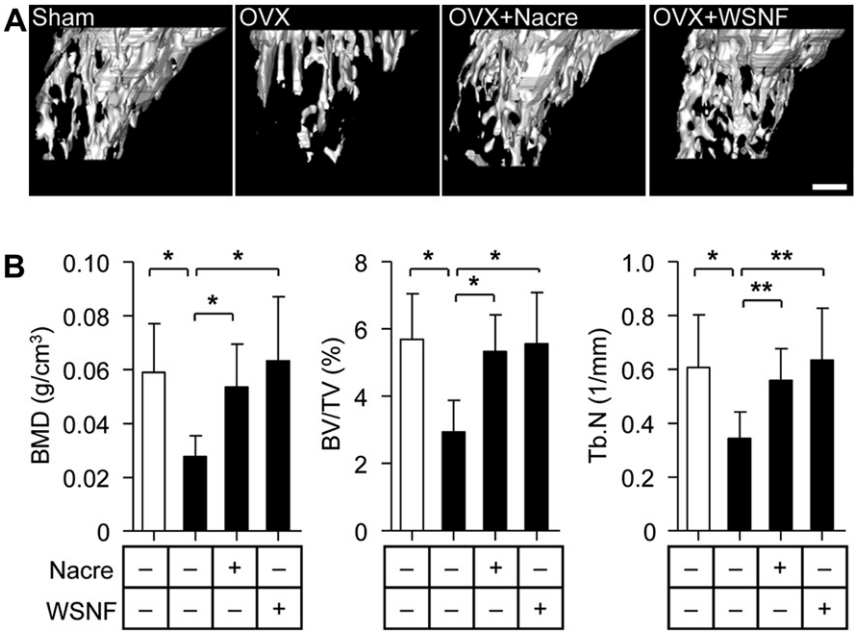

Fig. 1. Powdered nacre and WSNF each prevent OVX-induced bone loss in mice. (A) Representative μCT images of tibial trabecular bone in sham-operated mice as well as in OVX mice either not treated or treated orally with powdered nacre or WSNF for 30 days. Scale bar, 0.5 mm □, Sham; ■, OVX. (B) Analysis of bone loss indices with the μCT data obtained from mice treated as in A. Data are means ± SD ($n = 6$ mice per group). $^{*}P < 0.05$, $^{**}P < 0.01$.

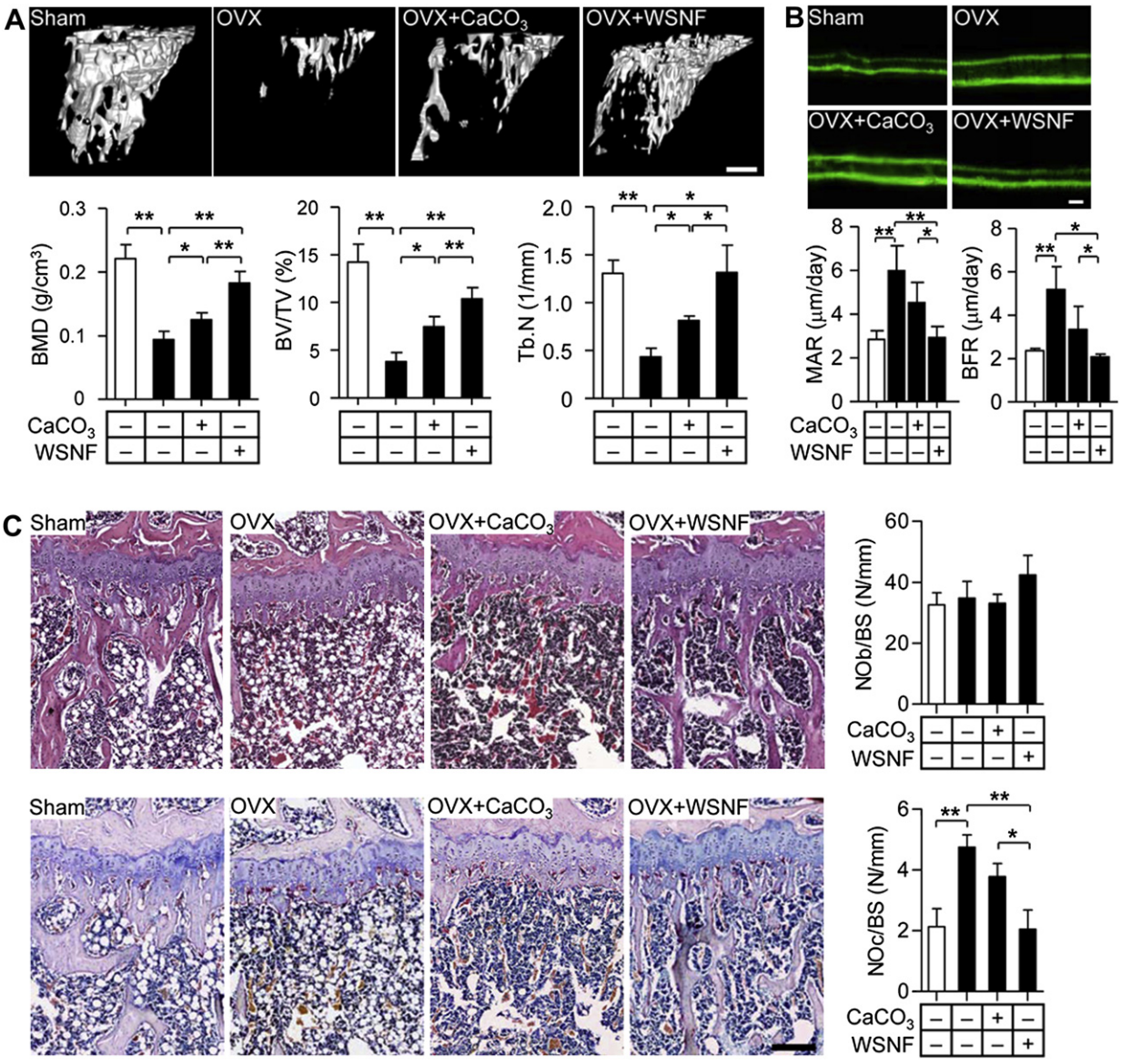

Fig. 2. WSNF promote osteoblast formation and inhibit osteoclast formation in OVX mice. (A) Representative μCT images of tibial trabecular bone as well as bone loss indices for sham-operated mice and OVX mice treated orally for 30 days with WSNF or with a solution containing an identical concentration of calcium dissolved from $CaCO_3$. Scale bar, 0.5 mm. (B) Mineral apposition rate (MAR) and bone formation rate (BFR) in the tibia were determined by the calcein double-labeling method for animals treated as in A. Representative images (upper) and quantitative data (lower) are shown. Scale bar, 10 μm. (C) Tibial sections from animals treated as in A were stained with hematoxylin–eosin (upper images) to detect osteoblasts and for tartrate-resistant acid phosphatase (TRAP) (lower images) to visualize osteoclasts, and the numbers of osteoblasts (NOb) and osteoclasts (NOc) per millimeter of trabecular bone surface (BS) were counted. Scale bar, 200 μm. All quantitative data are means ± SD ($n = 6$ mice per group). $^{*}P < 0.05$, $^{**}P < 0.01$. □, Sham; ■, OVX.

bone loss by WSNF is achieved mainly through inhibition of osteoclast formation.

3.3. Assessing osteoblast biomineralization in vitro

We next examined whether WSNF might potentiate osteoblast formation in an osteogenic culture system *in vitro*. The extents of mineralization and nodule formation, which reflect osteoblast differentiation, were visualized by staining with alizarin red S and were quantified by measurement of absorbance of the red dye eluted after staining. Osteoblast cultures exposed to WSNF showed a marked increase in the extent of calcification when compared with those exposed to water or calcium (Fig. 3A), but not osteoblast proliferation (Supplementary Fig. S1). To investigate further the effect of WSNF on osteoblast differentiation, we measured the enzymatic activity and expression of alkaline phosphatase (ALP), which are up-regulated at an early stage of mineralization [27]. Immunoblot analysis of osteoblast cultures revealed that the amount of ALP protein was increased markedly by WSNF treatment, whereas RT-PCR analysis showed that the abundance of ALP mRNA was unaffected (Supplementary Fig. S2). ALP activity was also significantly increased in the WSNF-treated cultures (Fig. 3B). These results indicated that WSNF increase ALP activity during osteoblast differentiation, most likely as a result of an effect (or effects) at the posttranscriptional level.

To identify possible mediators of WSNF-induced osteoblastogenesis, we examined various signaling molecules that are necessary for osteoblast differentiation. RT-PCR analysis showed that the amounts of mRNAs for transcription factors required for the osteoblastic phenotype, such as RUNX2 (encoded by *Cbfa1*) and

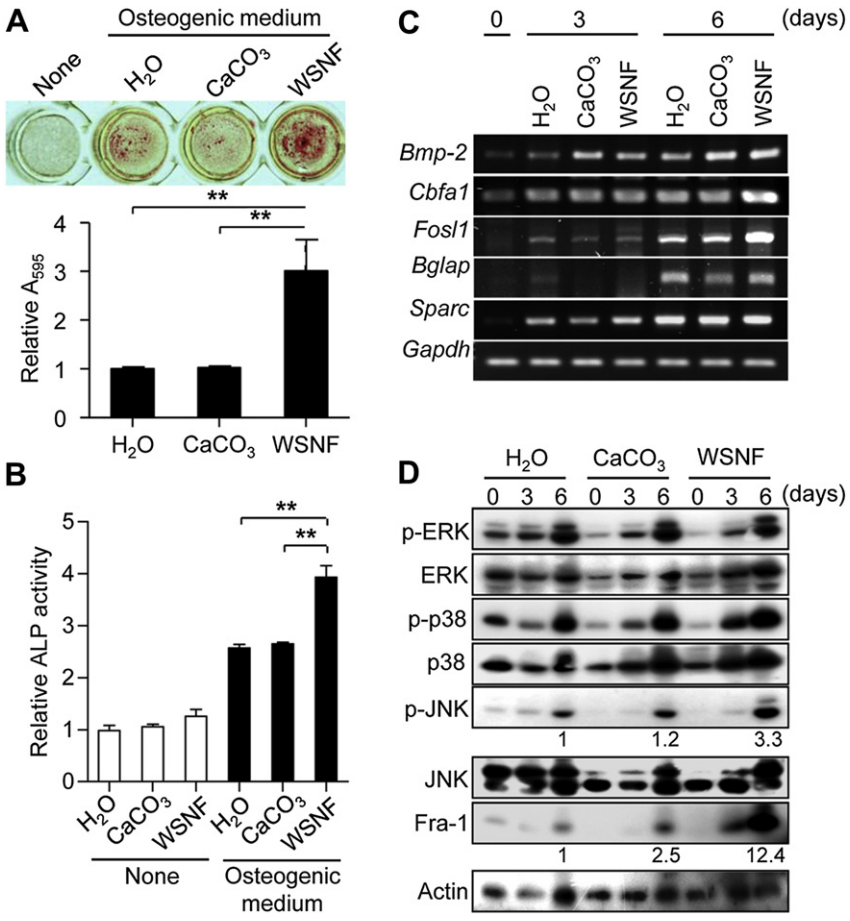

Fig. 3. WSNF stimulate osteoblast biomineralization *in vitro*. (A) Primary calvarial osteoblast precursors were cultured in osteogenic medium for 6 days in the absence or presence of WSNF or of either the same concentration of calcium dissolved from $CaCO_3$ as that provided by WSNF or of H_2O as controls. The cells were then stained with alizarin red S for detection of mineralized nodule formation (upper). For quantification of mineralization, alizarin red S was eluted with cetylpyridinium chloride and absorbance of the dye at 595 nm was measured (lower). (B) Cells treated as in A but cultured in osteogenic or normal medium were assayed for ALP activity. Quantitative data in A and B are means ± SD from three independent experiments. $^{**}P < 0.01$. (C) Total RNA isolated from cells cultured as in A for 0, 3, or 6 days was subjected to RT-PCR analysis of the indicated mRNAs. (D) Cells cultured as in A for 0, 3, or 6 days were subjected to immunoblot analysis with antibodies to total or phosphorylated (p−) forms of ERK, p38, or JNK or to Fra-1 or actin (loading control). Band intensities of the phosphorylated JNK and the Fra-1 for the 6-day cultures were represented as a fold difference relative to H_2O-treated control.

Fos-related antigen-1 (Fra-1, encoded by *Fosl1*), were increased by WSNF treatment, whereas those of mRNAs for the osteogenic growth factor BMP-2 (bone morphogenetic protein-2) and for the bone matrix proteins osteocalcin (encoded by *Bglap*) and osteonectin (encoded by *Sparc*) were not (Fig. 3C). In addition, immunoblot analysis revealed that, among mitogen-activated protein kinases (MAPKs), WSNF increased the phosphorylation of c-Jun NH_2-terminal kinase (JNK) without affecting that of extracellular signal-regulated kinase (ERK) or p38 (Fig. 3D). WSNF also increased the abundance of Fra-1, a downstream target of JNK signaling [28] (Fig. 3D). Together, these results suggested that activation of the JNK-Fra-1 axis may play a central role in the stimulatory effect of WSNF on the mineralization process of osteoblasts. Furthermore, WSNF are expected to contain water-soluble diffusible factors that can stimulate biomineralized function of osteoblasts *in vivo*.

3.4. Assessing osteoclast and bone pit formation in vitro

Given that the increased osteoclast formation in OVX mice was inhibited by administration of WSNF (Fig. 2C), we next tested whether WSNF inhibit the differentiation of bone marrow-derived mononuclear cells into functional multinucleated osteoclasts *in vitro*. The cells were cultured in the presence of both RANKL, an essential factor for osteoclast formation, and macrophage colony-stimulating factor (M-CSF), which supports the proliferation and survival of osteoclast precursors. WSNF inhibited the formation of TRAP-positive multinucleated cells, which correspond to mature osteoclasts capable of degrading bone (Fig. 4A), whereas WSNF did not affect the number of $TRAP^+$ mononuclear pre-osteoclasts (Supplementary Fig. S3) or the enzymatic activity of TRAP at the early stages of osteoclastogenesis (Fig. 4B). TRAP activity was decreased in the presence of WSNF at the later stages of this process associated with the appearance of multinucleated osteoclasts. The reduction in the number of mature osteoclasts formed in the presence of WSNF was not due to an effect on cell survival, given that the number of pre-osteoclasts was not affected. These results thus indicated that WSNF attenuate the formation of mature osteoclasts but not that of pre-osteoclasts. Consistent with these findings, the abundance of mRNAs for osteoclastic marker genes (*Acp5*, *Oscar*, *Car2*) as well as for the transcription factors c-Fos and NFATc1 (nuclear factor of activated T cells cytoplasmic 1), which are essential for mature osteoclast formation, was down-regulated by WSNF treatment (Fig. 4C).

To investigate the molecular mechanism underlying the inhibitory effect of WSNF on osteoclast formation, we examined early and late RANKL signaling. Immunoblot analysis revealed that WSNF suppressed RANKL-induced late responses including the up-regulation of c-Fos and NFATc1 [29,30] (Fig. 4D), whereas they did

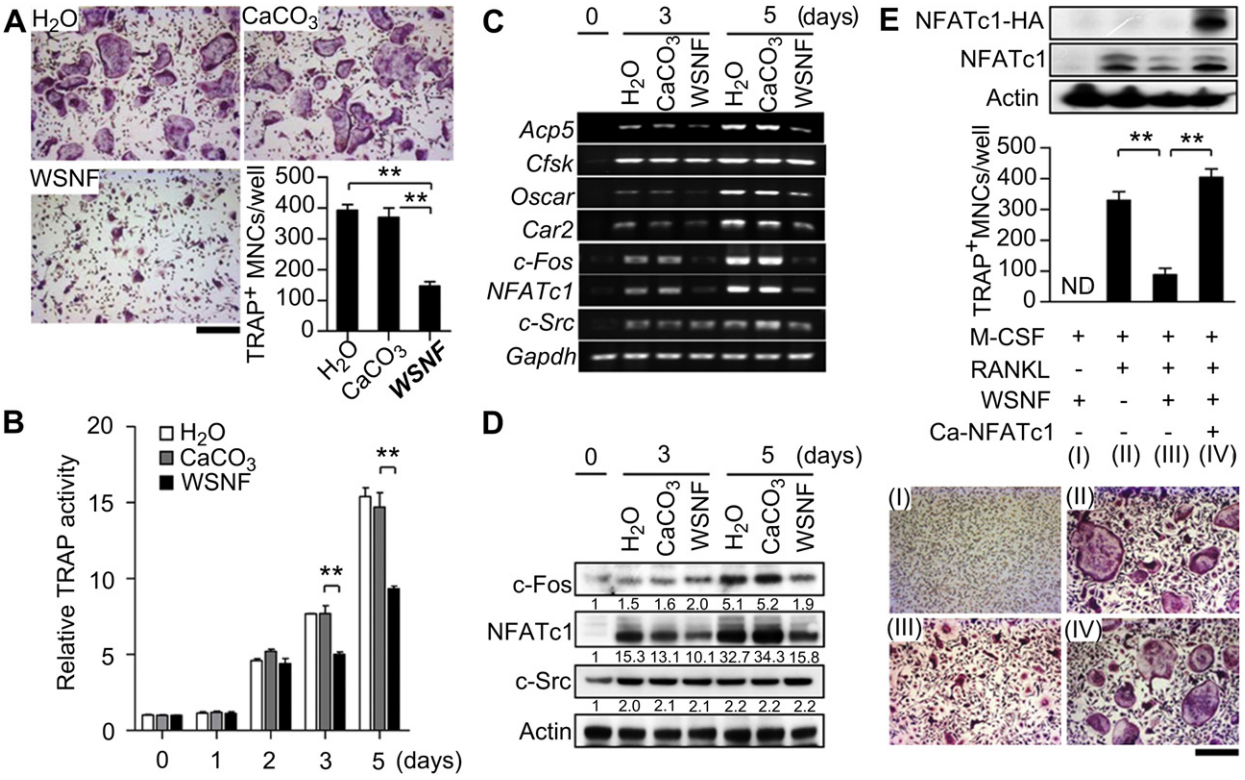

Fig. 4. WSNF inhibit osteoclast formation by attenuating the up-regulation of NFATc1. (A) Bone marrow–derived osteoclast precursors were cultured for 5 days with WSNF, $CaCO_3$, or H_2O as well as in the presence of M-CSF and RANKL to induce osteoclast formation. The cells were then fixed and stained for TRAP, and the number of $TRAP^+$ multinucleated (≥10 nuclei) cells (MNCs) was counted with a light microscope. Scale bar, 100 μm. (B) Cells treated as in A for the indicated times were assayed for TRAP activity. Quantitative data as in A and B are means ± SD from three independent experiments. $^{**}P < 0.01$. Cells incubated as in A for 0, 3, or 5 days were assayed for the indicated mRNAs by RT-PCR analysis (C) or subjected to immunoblot analysis with antibodies to the indicated proteins (D). Relative intensities of the c-Fos, NFATc1, and c-Src protein bands were determined by densitometry. (E) Osteoclast precursors infected with a retrovirus encoding an HA–tagged constitutively active form of NFATc1 (Ca-NFATc1) or with a control retrovirus were induced to differentiate into osteoclasts by culture for 5 days with M-CSF and RANKL and in the absence or presence of WSNF. The cells were then subjected to immunoblot analysis with antibodies to HA and to NFATc1 (upper) and were stained for TRAP (lower). $TRAP^+$ multinucleated cells were also counted (middle). Scale bar, 100 μm. Quantitative data are means ± SD from three independent experiments. $^{**}P < 0.01$. ND, not detected.

not affect RANKL-induced early signaling such as the activation of MAPKs (ERK, p38, JNK) and phosphorylation of the nuclear factor-κB (NF-κB) inhibitor Iκ-Bα (Supplementary Fig. S4). To determine whether overexpression of the osteoclastogenic master regulator NFATc1 was able to prevent the inhibition of osteoclast formation by WSNF, we infected osteoclast precursors with a retrovirus encoding a constitutively active form of NFATc1 prior to WSNF treatment. The inhibitory effect of WSNF on osteoclast formation was indeed prevented by forced expression of NFATc1 (Fig. 4E).

Finally, we measured the bone-resorbing capacity of mature osteoclasts in the presence of WSNF. The resorbed area of pits formed by mature osteoclasts on dentine slices was markedly reduced by the addition of WSNF (Fig. 5A). Multinucleated giant osteoclasts with a full actin ring were also transformed into cells with an irregular and condensed morphology in the presence of WSNF, resulting in a reduction in the number of mature osteoclasts capable of degrading bone. Together, our results thus indicated that WSNF both inhibit osteoclast maturation by attenuating the up-regulation of NFATc1 as well as suppress osteoclast function by disrupting the actin ring, a cytoskeletal structure that is important for formation of the sealing zone required for bone mineral dissolution and bone matrix protein degradation by osteoclasts [31].

4. Discussion

The ultimate goal in the development of anti-osteoporotic agents is bone improvement by simultaneous osteoblast stimulation and osteoclast inhibition and with no undesirable side effects. To achieve this goal, we have examined natural materials for such anti-osteoporotic agents. In the present study, we selected nacre, which is functionally and microstructurally similar to human bone [32] and is used as a traditional treatment for osteoporosis in oriental medicine, as such a natural material for characterization. Our findings suggest that WSNF both inhibit the differentiation and resorptive function of osteoclasts and stimulate mineralization by osteoblasts (Fig. 5C).

Hard tissue biomineralization results in the formation of a skeleton composed of calcium phosphate in vertebrates and in that of a shell composed of calcium carbonate in invertebrates [15,33]. Bone comprises 30–40% organic matrix, which is composed mainly of type I collagen, and 60–70% mineral salts [14]. New bone is synthesized by biomineralization of osteoblast-derived membrane-bound matrix vesicles, and old bone is removed by dissolution of minerals and degradation of the organic matrix by osteoclasts [2], with ~10% of bone in adult humans being replaced each year. Nacre, one of the layers of the pearl oyster shell, differs from bone in terms of the mineralization process and composition. It thus comprises 1–5% organic matrix and 95–99% minerals, and it is synthesized by the deposition of calcium carbonate within the organic protein matrix [13,15]. Although the nacreous layer formation is known, there is no evidence for nacre destruction [34,35]. Nacre is similar to bone, however, in terms of its basic higher-order layered microstructure and protective function.

Despite the differences between bone and nacre, we have now found that WSNF ameliorated osteoporotic bone loss associated

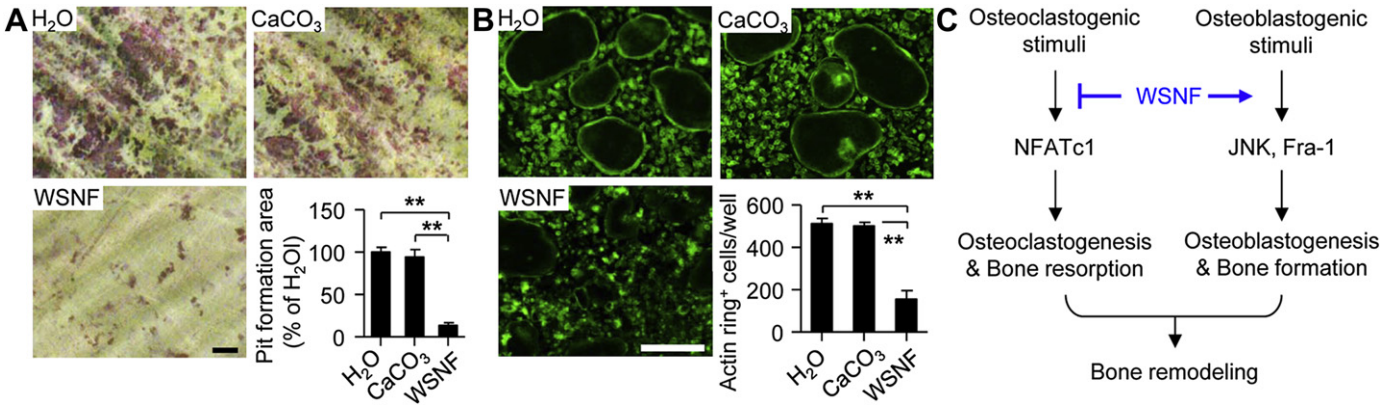

Fig. 5. WSNF inhibit pit formation by osteoclasts and disrupt the actin ring in these cells. (A) Bone marrow-derived osteoclast precursors were cultured on dentine slices for 5 days with M-CSF and RANKL to induce differentiation into mature osteoclasts and were then incubated for 2 days in the additional presence of WSNF, $CaCO_3$, or H_2O. The cells were then removed and the dentine slices were stained with hematoxylin for measurement of the resorbed area. Scale bar, 100 μm. (B) Mature osteoclasts were incubated for 2 days with WSNF, $CaCO_3$, or H_2O in the presence of M-CSF and RANKL, fixed, permeabilized, stained with fluorescein isothiocyanate-conjugated phalloidin, and examined by fluorescence microscopy. Mature osteoclasts with a full actin ring were counted. Scale bar, 100 μm. Quantitative data in A and B are means ± SD from three independent experiments. $^{**}P < 0.01$. (C) Proposed schematic representation for the beneficial effect of WSNF on bone remodeling.

with estrogen deficiency in mice mainly through osteoclast inactivation and possibly through osteoblast activation. Nacre has been shown to contain osteogenic factors ranging from small inorganic and organic components to large matrix proteins [19,20,36–39]. Low molecular weight molecules ranging from 50 to 235 Da and relatively high molecular weight organic matrix proteins present in nacre have thus been found to promote osteogenesis both directly through stimulation of osteoblast function and indirectly by inducing the synthesis of fibrous matrix proteins including type I collagen by fibroblasts [36–40]. We also found that WSNF include calcium and phosphate, which can potentiate osteoblast mineralization [41], and unknown proteinaceous components. Treatment with calcium at a final concentration of 14 μM,, which was the same concentration of calcium containing WSNF, did not affect biomineralization *in vitro* (Fig. 3A and Supplementary Fig. S5). In contrast, calcium at a concentration identical to that dissolved in WSNF induced a slight increase in bone formation *in vivo* (Fig. 2A) and osteoblast mineralization by calcium was enhanced in a dose dependent manner *in vitro* (Supplementary Fig. S5). In addition, treatment with phosphate at a concentration identical to that dissolved in WSNF did not affect osteoblast mineralization *in vitro* (data not shown). These results indicate that WSNF are likely to contain water-soluble diffusible factors that can stimulate osteoblasts *in vivo* and the prevention of bone loss by WSNF was likely due to the combined effects of calcium and unknown water-soluble factors. Taken together, the stimulatory action of WSNF on bone formation is believed to help the serial process of osteoblastic matrix formation and mineral deposition.

Our data suggest that WSNF inhibit osteoclast maturation and bone resorption by respectively preventing the up-regulation of NFATc1 and inducing disruption of the actin ring that forms at the sealing zone of active osteoclasts and is critical for bone resorption. Remodeling of the actin cytoskeleton in osteoclasts is regulated by a signaling pathway including integrin $\alpha_v\beta_3$, phosphoinositide 3-kinase, and the Rho GTPase [42]. Recent reports including our previous study showed that a novel cell-permeable peptide directly modulates formation of the sealing ring by osteoclasts [43,44]. These observations suggest that WSNF may contain specific molecules that restrict mature osteoclast formation and destabilize the actin ring in these cells and thereby inhibit their function. Moreover, the combined results indicate that WSNF are likely to contain bone remodeling factors with various molecular weights, ranging from small inorganic and organic compounds to large matrix proteins [22], and the beneficial effect of WSNF on osteoporosis may be caused by the combination between the previously identified and unknown materials. Combination therapy with two or more drugs often achieves the same therapeutic effect as that achieved by monotherapy but at doses of each agent lower than those effective in monotherapy and therefore with reduced side effects. Thus, when nacreous mixtures is fractionated to identify a particular molecule and then applied to clinical application, the prudential combination between individual batches is required to improve bone remodeling by simultaneously inhibiting osteoclastic bone resorption as well as stimulating osteoblastic bone formation.

Newly synthesized bone forms around implanted nacre, and nacre particles are slowly dissolved by active osteoclasts in bone with limited degradation [40,45]. Furthermore, the biomineralization induced by and biodegradation of nacre progress without an inflammatory reaction [40,45]. Nacre has been proposed to contain diffusible bioactive factors that are able to initiate osteogenesis by stimulating the synthesis of extracellular matrix proteins in fibroblasts adjacent to the implant area [37–39]. We recently also found that nacreous factors accelerate the healing of skin wounds by facilitating the production of collagenous matrix protein by fibroblasts [22]. Osteogenic matrix proteins generated by fibroblasts in the dermis may also promote the regeneration of bone tissue adjacent to the dermis. Given that nacre becomes integrated into bone with biocompatibility and contains bioactive osteogenic factors [16,40,46–48], it may be suitable for the future development of advanced bone materials. We found that powdered nacre and WSNF exhibited similar effects in preventing osteoporosis associated with estrogen deficiency. WSNF may prove more suitable as a therapeutic agent than powdered nacre, however, as a result of superior biocompatibility. Among various nacreous forms, both WSNF and powdered form of nacre are allowed for a systemic clinical approach via oral administration. WSNF may be more suitable than powdered nacre when applied to a wounded part like skin injury caused by burns and powdered nacre may be more favorable than WSNF for developing bone-mimetic materials when implanted *in vivo*. Based on our previous [22] and present observations as well as the anecdotal evidence of an experienced doctor of oriental medicine, we here suggest that the recommended daily intake of nacre to improve osteoporotic bone loss in adult humans is approximately 25 mg/kg.

5. Conclusions

The development of therapeutic agents for osteoporosis is ultimately required to prevent bone resorption and to enhance bone formation. However, uncoupling agents that display antiresorptive and anabolic functions have not yet been developed. In this regard, we have now shown that a natural material–derived preparation, WSNF, modulates bone remodeling by inhibiting osteoclast differentiation and function and stimulating osteoblast function. These effects resulted in prevention of osteoporotic bone loss associated with estrogen deficiency in mice. Further studies are warranted to apply nacreous factors to the development of bone substitutes and anti-osteoporotic agents for humans.

Acknowledgments

We thank J. S. Bae (Uiseong Oriental Medicine Hospital, Korea) for helpful discussion on the clinical efficacy of nacre. This work was supported, in part, by grants from the Korea Healthcare Technology R&D Project, Ministry for Health, Welfare & Family Affairs, Republic of Korea (no. A084221 to DJ) and from the National Research Foundation of Korea (nos. 2011-0006178 to DJ and 2011-0002984 to SHL).

Appendix A. Supplementary material

Supplementary material associated with this article can be found, in the online version, at http://dx.doi.org/10.1016/j.biomaterials.2012.06.098.

References

[1] Grabowski P. Physiology of bone. Endocr Dev 2009;16:32–48.
[2] Kartsogiannis V, Ng KW. Cell lines and primary cell cultures in the study of bone cell biology. Mol Cell Endocrinol 2004;228:79–102.
[3] Walsh MC, Kim N, Kadono Y, Rho J, Lee SY, Lorenzo J, et al. Osteoimmunology: interplay between the immune system and bone metabolism. Annu Rev Immunol 2006;24:33–63.
[4] Ishida A, Fujita N, Kitazawa R, Tsuruo T. Transforming growth factor-beta induces expression of receptor activator of NF-kappa B ligand in vascular endothelial cells derived from bone. J Biol Chem 2002;277:26217–24.
[5] Matsuo K, Irie N. Osteoclast-osteoblast communication. Arch Biochem Biophys 2008;473:201–9.
[6] Liu HY, Wu AT, Tsai CY, Chou KR, Zeng R, Wang MF, et al. The balance between adipogenesis and osteogenesis in bone regeneration by platelet-rich plasma for age-related osteoporosis. Biomaterials 2011;32:6773–80.
[7] Zaidi M. Skeletal remodeling in health and disease. Nat Med 2007;13:791–801.
[8] Jerome CP, Carlson CS, Register TC, Bain FT, Jayo MJ, Weaver DS, et al. Bone functional changes in intact, ovariectomized, and ovariectomized, hormone-supplemented adult cynomolgus monkeys (Macaca fascicularis) evaluated by serum markers and dynamic histomorphometry. J Bone Miner Res 1994;9:527–40.
[9] Baldock PA, Morris HA, Need AG, Moore RJ, Durbridge TC. Variation in the short-term changes in bone cell activity in three regions of the distal femur immediately following ovariectomy. J Bone Miner Res 1998;13:1451–7.
[10] Jilka RL, Weinstein RS, Takahashi K, Parfitt AM, Manolagas SC. Linkage of decreased bone mass with impaired osteoblastogenesis in a murine model of accelerated senescence. J Clin Invest 1996;97:1732–40.
[11] Kawaguchi H, Manabe N, Miyaura C, Chikuda H, Nakamura K, Kuro-o M. Independent impairment of osteoblast and osteoclast differentiation in klotho mouse exhibiting low-turnover osteopenia. J Clin Invest 1999;104:229–37.
[12] Levi-Kalisman Y, Falini G, Addadi L, Weiner S. Structure of the nacreous organic matrix of a bivalve mollusk shell examined in the hydrated state using cryo-TEM. J Struct Biol 2001;135:8–17.
[13] Weiner S. Organization of extracellularly mineralized tissues: a comparative study of biological crystal growth. CRC Crit Rev Biochem 1986;20:365–408.
[14] Boivin G, Meunier PJ. Effects of bisphosphonates on matrix mineralization. J Musculoskelet Neuronal Interact 2002;2:538–43.
[15] Furuhashi T, Schwarzinger C, Miksik I, Smrz M, Beran A. Molluscan shell evolution with review of shell calcification hypothesis. Comp Biochem Physiol B Biochem Mol Biol 2009;154:351–71.
[16] Liao H, Brandsten C, Lundmark C, Wurtz T, Li J. Responses of bone to titania-hydroxyapatite composite and nacreous implants: a preliminary comparison by in situ hybridization. J Mater Sci Mater Med 1997;8:823–7.
[17] Berland S, Delattre O, Borzeix S, Catonne Y, Lopez E. Nacre/bone interface changes in durable nacre endosseous implants in sheep. Biomaterials 2005;26:2767–73.
[18] Atlan G, Balmain N, Berland S, Vidal B, Lopez E. Reconstruction of human maxillary defects with nacre powder: histological evidence for bone regeneration. C R Acad Sci III 1997;320:253–8.
[19] Rousseau M, Pereira-Mouries L, Almeida MJ, Milet C, Lopez E. The water-soluble matrix fraction from the nacre of Pinctada maxima produces earlier mineralization of MC3T3-E1 mouse pre-osteoblasts. Comp Biochem Physiol B Biochem Mol Biol 2003;135:1–7.
[20] Mouries LP, Almeida MJ, Milet C, Berland S, Lopez E. Bioactivity of nacre water-soluble organic matrix from the bivalve mollusk Pinctada maxima in three mammalian cell types: fibroblasts, bone marrow stromal cells and osteoblasts. Comp Biochem Physiol B Biochem Mol Biol 2002;132:217–29.
[21] Duplat D, Gallet M, Berland S, Marie A, Dubost L, Rousseau M, et al. The effect of molecules in mother-of-pearl on the decrease in bone resorption through the inhibition of osteoclast cathepsin K. Biomaterials 2007;28:4769–78.
[22] Lee K, Kim H, Kim JM, Chung YH, Lee TY, Lim HS, et al. Nacre-driven water-soluble factors promote wound healing of the deep burn porcine skin by recovering angiogenesis and fibroblast function. Mol Biol Rep 2012;39:3211–8.
[23] Sakai A, Nishida S, Okimoto N, Okazaki Y, Hirano T, Norimura T, et al. Bone marrow cell development and trabecular bone dynamics after ovariectomy in ddy mice. Bone 1998;23:443–51.
[24] Lee SH, Rho J, Jeong D, Sul JY, Kim T, Kim N, et al. v-ATPase V0 subunit d2-deficient mice exhibit impaired osteoclast fusion and increased bone formation. Nat Med 2006;12:1403–9.
[25] Lee SH, Kim T, Jeong D, Kim N, Choi Y. The tec family tyrosine kinase Btk regulates RANKL-induced osteoclast maturation. J Biol Chem 2008;283:11526–34.
[26] Rachner TD, Khosla S, Hofbauer LC. Osteoporosis: now and the future. Lancet 2011;377:1276–87.
[27] Bonucci E, Silvestrini G, Bianco P. Extracellular alkaline phosphatase activity in mineralizing matrices of cartilage and bone: ultrastructural localization using a cerium-based method. Histochemistry 1992;97:323–7.
[28] Krum SA, Chang J, Miranda-Carboni G, Wang CY. Novel functions for NFkappaB: inhibition of bone formation. Nat Rev Rheumatol 2010;6:607–11.
[29] Grigoriadis AE, Wang ZQ, Cecchini MG, Hofstetter W, Felix R, Fleisch HA, et al. c-Fos: a key regulator of osteoclast-macrophage lineage determination and bone remodeling. Science 1994;266:443–8.
[30] Takayanagi H, Kim S, Koga T, Nishina H, Isshiki M, Yoshida H, et al. Induction and activation of the transcription factor NFATc1 (NFAT2) integrate RANKL signaling in terminal differentiation of osteoclasts. Dev Cell 2002;3:889–901.
[31] Wilson SR, Peters C, Saftig P, Bromme D. Cathepsin K activity-dependent regulation of osteoclast actin ring formation and bone resorption. J Biol Chem 2009;284:2584–92.
[32] Tang Z, Kotov NA, Magonov S, Ozturk B. Nanostructured artificial nacre. Nat Mater 2003;2:413–8.
[33] Murdock DJ, Donoghue PC. Evolutionary origins of animal skeletal biomineralization. Cells Tissues Organs 2011;194:98–102.
[34] Lowenstam HA. Minerals formed by organisms. Science 1981;211:1126–31.
[35] Fang D, Xu G, Hu Y, Pan C, Xie L, Zhang R. Identification of genes directly involved in shell formation and their functions in pearl oyster, Pinctada fucata. PLoS One 2011;6:e21860.
[36] Rousseau M, Boulzaguet H, Biagianti J, Duplat D, Milet C, Lopez E, et al. Low molecular weight molecules of oyster nacre induce mineralization of the MC3T3-E1 cells. J Biomed Mater Res A 2008;85:487–97.
[37] Lopez E, Le Faou A, Borzeix S, Berland S. Stimulation of rat cutaneous fibroblasts and their synthetic activity by implants of powdered nacre (mother of pearl). Tissue Cell 2000;32:95–101.
[38] Lopez E, Vidal B, Berland S, Camprasse S, Camprasse G, Silve C. Demonstration of the capacity of nacre to induce bone formation by human osteoblasts maintained in vitro. Tissue Cell 1992;24:667–79.
[39] Silve C, Lopez E, Vidal B, Smith DC, Camprasse S, Camprasse G, et al. Nacre initiates biomineralization by human osteoblasts maintained in vitro. Calcif Tissue Int 1992;51:363–9.
[40] Westbroek P, Marin F. A marriage of bone and nacre. Nature 1998;392:861–2.
[41] Mahamid J, Sharir A, Gur D, Zelzer E, Addadi L, Weiner S. Bone mineralization proceeds through intracellular calcium phosphate loaded vesicles: a cryo-electron microscopy study. J Struct Biol 2011;174:527–35.
[42] Ross FP, Teitelbaum SL. alphavbeta3 and macrophage colony-stimulating factor: partners in osteoclast biology. Immunol Rev 2005;208:88–105.
[43] Ma T, Samanna V, Chellaiah MA. Dramatic inhibition of osteoclast sealing ring formation and bone resorption in vitro by a WASP-peptide containing pTyr294 amino acid. J Mol Signal 2008;3:4.
[44] Kim H, Choi HK, Shin JH, Kim KH, Huh JY, Lee SA, et al. Selective inhibition of RANK blocks osteoclast maturation and function and prevents bone loss in mice. J Clin Invest 2009;119:813–25.
[45] Duplat D, Chabadel A, Gallet M, Berland S, Bedouet L, Rousseau M, et al. The in vitro osteoclastic degradation of nacre. Biomaterials 2007;28:2155–62.
[46] Dupoirieux L, Costes V, Jammet P, Souyris F. Experimental study on demineralized bone matrix (DBM) and coral as bone graft substitutes in maxillofacial surgery. Int J Oral Maxillofac Surg 1994;23:395–8.
[47] Liao H, Mutvei H, Sjostrom M, Hammarstrom L, Li J. Tissue responses to natural aragonite (Margaritifera shell) implants in vivo. Biomaterials 2000;21:457–68.
[48] Bahar H, Yaffe A, Binderman I. The influence of nacre surface and its modification on bone apposition: a bone development model in rats. J Periodontol 2003;74:366–71.